Evaluation of non-rigid constrained CT/CBCT registration algorithms for delineation propagation in the context of prostate cancer radiotherapy

Mathieu Rubeaux[ab] and Antoine Simon[ab] and Khemara Gnep[c] and Jérémy Colliaux[c] and Oscar Acosta[ab] and Renaud de Crevoisier[abc] and Pascal Haigron[ab]

[a]INSERM, UMR 1099, Rennes, F-35000, France;
[b]Université de Rennes 1, LTSI, F-35000, France;
[c] Département de Radiothérapie, Centre Eugène Marquis, Rennes, F-35000, France

ABSTRACT

Image-Guided Radiation Therapy (IGRT) aims at increasing the precision of radiation dose delivery. In the context of prostate cancer, a planning Computed Tomography (CT) image with manually defined prostate and organs at risk (OAR) delineations is usually associated with daily Cone Beam Computed Tomography (CBCT) follow-up images. The CBCT images allow to visualize the prostate position and to reposition the patient accordingly. They also should be used to evaluate the dose received by the organs at each fraction of the treatment. To do so, the first step is a prostate and OAR segmentation on the daily CBCTs, which is very time-consuming. To simplify this task, CT to CBCT non-rigid registration could be used in order to propagate the original CT delineations in the CBCT images. For this aim, we compared several non-rigid registration methods. They are all based on the Mutual Information (MI) similarity measure, and use a BSpline transformation model. But we add different constraints to this global scheme in order to evaluate their impact on the final results. These algorithms are investigated on two real datasets, representing a total of 70 CBCT on which a reference delineation has been realized. The evaluation is led using the Dice Similarity Coefficient (DSC) as a quality criteria. The experiments show that a rigid penalty term on the bones improves the final registration result, providing high quality propagated delineations.

Keywords: Image-Guided Radiation Therapy, prostate cancer, CT/CBCT registration, delineation propagation

1. PURPOSE

Prostate cancer is the most recurrent cancer for men. All prostate cancers can be treated by radiotherapy. But the clinical efficiency of this treatment may be dramatically limited by anatomic variations occurring during treatment. Indeed, the dose distribution is defined on one planning CT (before treatment), while the dose is delivered in several (e.g. 40) treatment fractions. At the same time, the prostate can move inside the pelvis up to 2 cm, exposing the prostate to a risk of under-dosage and therefore the patient to an increased risk of tumor recurrence. In the same way, the bladder and the rectum (organs at risk (OAR)) may present significant deformations (shape and volume variations due to bladder and rectum filling variations) leading to a received dose that may significantly differ from the planned one and exposing the patient to an increased risk of toxicity.

Image Guided Radiotherapy (IGRT) aims at increasing the precision of radiation dose delivery. In the context of prostate cancer, a planning CT image with manually defined prostate and OAR delineations is usually associated with daily CBCT follow-up images. The CBCT images allow to visualize the prostate position and to reposition the patient accordingly. However, this process can not correct for OAR deformations.

Further author information: (Send correspondence to Mathieu Rubeaux)
Mathieu Rubeaux: E-mail: mrubeaux@gmail.com, Telephone: +33 (0)6 27 95 36 22
Antoine Simon: E-mail: antoine.simon@univ-rennes1.fr, Telephone: +33 (0)2 23 23 62 20

In order to be able compute the dose actually received by the organs at one given fraction, the CBCT delineation is mandatory. However the expert manual delineation is too time-consuming to be considered in a clinical routine. Moreover, because of the poor quality of the CBCT images (very low contrast, noise,...), the classical segmentation methods tend to fail. In this context, image registration may be used to estimate the tissue deformation in order to propagate the CT delineations into the CBCT domain, allowing automatic delineation of the prostate and OAR on the CBCT images. But due to the poor quality of CBCT images and to the occurence of large deformations, this step still remains challenging. Some approaches have already been proposed[1,2] which combine non-rigid registration and segmentation in order to propagate CT delineations in the CBCT images.

In this study, we compare several iconic registration methods using the MI similarity measure. These methods are led in two steps: first, a rigid registration is performed, which serves as a preprocessing step for the non-rigid registration. This non-rigid registration step is performed using B-Splines as a deformation model. Moreover, two different constraint energies are added to the registration scheme and compared. The first one insures the global smoothness of the transformation to prevent undesired foldings, while the second one considers the rigidity of the bones structures in the area near the main considered organs. The experiments are realized on real data, and the Dice score is chosen as quality criterion.

This paper is organized as follows: section 2 gives technicals choices regarding the registration methods that are compared. The accent is put on the constraint energies that are employed. Then section 3 gives the results obtained from the different registration procedures. Finally a conclusion is given in section 4.

2. METHODS

An iconic registration scheme, based on the grey values of the pixels of the images to register, is applied. A registration method is usually defined by i) a similarity measure, ii) a motion model and iii) an optimization procedure. We define above the choices we made regarding this components in the study. The elastiX toolbox[3] is used during the registration procedures, which allows the reproducibility of the results by the use of parameter files.

2.1 Similarity measure

Let $I_F(\boldsymbol{\nu})$ be the CT floating image we want to register to a reference CBCT image $I_R(\boldsymbol{\nu})$, where $\boldsymbol{\nu}$ is a random vector over coordinate locations in the model. For the sake of convenience, let's define a vector $\boldsymbol{x}$ of two random variables $x^{(1)}$ and $x^{(2)}$, which will denote $I_F(\boldsymbol{\nu})$ and $I_R(\boldsymbol{\nu})$, respectively. The Mutual Information (MI) similarity measure is chosen, since it allows efficient multimodal registration. It can be expressed as a function of the marginal and joint entropies of $x^{(1)}$ and $x^{(2)}$:

$$MI(\boldsymbol{x}) = H(x^{(1)}) + H(x^{(2)}) - H(\boldsymbol{x}) \tag{1}$$

Moreover, Mattes[4,5] implementation of MI is used, which is based on a compact B-Spline kernel. Indeed, it allows to take into account a small amount of the voxels of the images to register to estimate the measure, and hence permits fast registration.

2.2 Constraint energies

Besides this similarity measure, the motion is regularized using two different methods:

(i) a penalty term based on the bending energy of a thin metal sheet[6] that insures the global smoothness of the transformation. One of the major difficulty with the CBCT images is the lack of information in the considered organs region. It is often hard to visually distinguish between the bladder and the prostate boundaries in some regions. This energy prevents the deformation field based on B-Splines to diverge in these areas, and is given by:

$$\begin{aligned} P_{BE} &= \frac{1}{V}\int_0^X\int_0^Y\int_0^Z\Bigg[\left(\frac{\partial^2\mathbf{T}}{\partial x^2}\right)^2+\left(\frac{\partial^2\mathbf{T}}{\partial y^2}\right)^2+\left(\frac{\partial^2\mathbf{T}}{\partial z^2}\right)^2+2\left(\frac{\partial^2\mathbf{T}}{\partial xy}\right)^2 \\ &+ 2\left(\frac{\partial^2\mathbf{T}}{\partial xz}\right)^2+2\left(\frac{\partial^2\mathbf{T}}{\partial yz}\right)^2\Bigg]dxdydz \end{aligned} \tag{2}$$

where V denotes the volume of the image domain, and $\mathbf{T}$ the considered transformation.

(ii) a rigid penalty term[7] on the bones that are extracted by thresholding the original image. This term forces the bones to deform rigidly during the non-rigid registration. On the images, the bones are very informative and the registration tends to be guided by these structures. By forcing their rigidity, it is possible to concentrate the deformation in the region of interest containing the prostate and the OARs.

In this study, three methods are compared, depending on wether a constraint is used or not: MI denotes the registration scheme without regularization, MI_{BE} stands for the registration with a Bending Energy penalty, while MI_{RP} indicates the procedure with a Rigid Penalty on the bones. When a constraint is used, the global similarity measure becomes a balanced sum of MI and of the considered penalty.

2.3 Motion model

Regarding the motion model, the registration procedure is divided in two steps: first, a rigid registration to globally align the two images; second, a non-rigid registration using a Free-Form Deformation (FFD) model based on B-Splines.[6] The FFD model warps an image by moving an underlying set of control points distributed over a regular grid. The displacement of a point $\boldsymbol{\nu}$ of the image can be written as a linear combination of B-Spline functions $\beta^{(k)}$, weighted by the parameters $\boldsymbol{\xi}^{(k)}$ (representing the displacement of the control points) in the neighborhood $\mathcal{K}(\boldsymbol{\nu})$ of this point:

$$\phi(\boldsymbol{\nu}, \boldsymbol{\xi}) = \sum_{k \in \mathcal{K}(\boldsymbol{\nu})} \boldsymbol{\xi}^{(k)} \beta^{(k)}(\boldsymbol{\nu}) \tag{3}$$

Finally, we choose a linear interpolation which is a good compromise beetwen efficiency and speed.

2.4 Optimization procedure

We use an adaptive stochastic gradient descent procedure described in,[8] given by:

$$\boldsymbol{\mu}_{k+1} = \boldsymbol{\mu}_k - \gamma(t_k)\,\tilde{\mathbf{g}}_k, \;\; k = 0, 1, \ldots, K \tag{4}$$

with $\boldsymbol{\mu}_k$ and $\boldsymbol{\mu}_{k+1}$ the transformation parameters at iteration k and $k+1$, respectively. The search direction $\tilde{\mathbf{g}}_k$ is the analytical derivative of the MI as defined in,[4,5] and the gain factor $\gamma(t_k)$ is determined by a predefined decaying function of the iteration number k:

$$\begin{aligned} \gamma(t_k) &= \frac{a}{(t_k + A)} \\ t_{k+1} &= \max[t_k + f(-\tilde{\mathbf{g}}_k^{\intercal}\tilde{\mathbf{g}}_{k-1}), 0] \end{aligned} \tag{5}$$

where f denotes a sigmoid function. The originality of this algorithm comes from the automatic estimation of the free parameters, namely a, A and f, before the registration starts. This estimation is done using the properties of both the images to register and the similarity measure used. Moreover, we choose a coarse to fine (or pyramidal) approach, which brings a speed-up in the registration.

During rigid registration procedure, the pyramidal approach consists in downsampling the images with a factor 2 at each level and performing the registration on the coarser level. When the optimum parameters are found, they are used to initialize the next level of the pyramid. In this study, four resolutions are used.

During the non-rigid registration, the downsampling is done both on the images and on the control grid of the B-Splines. The process starts with a coarse grid which is refined after the optimum is reached. This approach gives faster and better results, because it allows us to register global as well as local motion. Three resolutions for both the images and the control grid pyramids are used. The final spacing between the B-Splines control points is 12mm. It is noteworthy that the non-rigid registration procedure is led on a Region Of Interest (ROI) around the prostate and OARs, as will be seen farther in this paper (figure 3 and 4). This ROI is automatically deduced from the expert segmentations on the CT, which are always available in clinical practice, and is applied to both the CT and the CBCT.

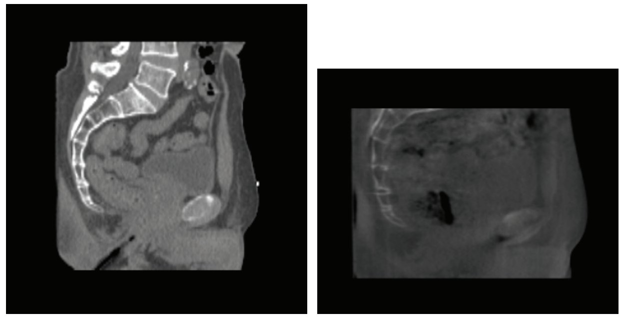

(a) CT (b) CBCT

Figure 1. Example of data used in this study. The CT moving image (a) is registered to each CBCT fixed image (b).

3. RESULTS

The data used in this study comes from the Centre Eugène Marquis in Rennes, France. It consists of 2 subjects who have been treated for a prostate cancer. For each subject a pre-treatment CT and some daily CBCT images are available. All the images (CT and CBCT) have been manually delineated by an expert to segment the prostate and OAR, allowing to compare the delineations obtained by the non-rigid registration algorithms with the one from the expert. For the first subject, 32 CBCTs are available while for the second, 38 images are given. An example of the data is given in figure 1. It shows the poor quality of CBCT images, which makes the registration procedure though.

Once the non-rigid registration procedure is performed, the dense deformation field that is obtained can be used to deform the CT expert delineations, in order to bring them in the CBCT domain, which in the final goal of this application. Since the CBCT expert delineations are also available, it is then possible to compare these CBCT delineations, with the ones produced by the registration procedure. The evaluation is then made using the DSC (Dice Similarity Coefficient) to assess the relevance of the non-rigid propagated delineations, compared to the existing expert ones. The results are given in figure 2 for the different organs under study. Regarding the different registration algorithms used, one can see that except for the bladder (figure 2(c)), the DSC always improves when a rigid penalty term is added to the MI.

Considering the results in detail, the average DSC for the prostate (figure 2(a)) over the 2 subjects is 0.81 (0.73-0.88) with MI, 0.82 (0.75-0.85) with MI_{BE} and 0.86 (0.74-0.90) with MI_{RP}. For the rectum (figure 2(b)), The average DSC is 0.6 (0.5-0.68) with MI, 0.6 (0.47-0.7) with MI_{BE} and 0.64 (0.53-0.76) with MI_{RP}. For the bladder (figure 2(c)), we obtained a DSC of 0.84 (0.66-0.93) with MI, 0.83 (0.62-0.93) with MI_{BE} and 0.81 (0.64-0.93) with MI_{RP}. And finally, the poorer results are obtained with the seminal vesicles (figure 2(d)), which are difficult to register dur to their small size and contrast. The DSC is then 0.42 (0.15-0.69) with MI, 0.44 (0.2-0.67) with MI_{BE} and 0.48 (0-0.7) with MI_{RP}.

The figure 3 gives an example of delineation propagation results for the bladder, compared to the reference expert delineation, using the 3 registration methods. All the delineations are superimposed on the fixed image to see the overlap between the found delineation and the real data. It demonstrates the difficulty to visually assess the quality of an automatic registration procedure, besides with three dimensionnal data, even if one can see that the results differ one compared to the other. It also shows that even if the DSC with MI_{RP} is somehow worse than the ones with MI and MI_{BE}, the propagated delineation with MI_{RP} seems closer to the expert ones. The same kind of results can be observed on figure 4, where the propagated prostate with the three presented methods is compared to the expert delineation, MI_{RP} giving better results.

4. CONCLUSION

In this preliminary study, the effect of different constraints for delineation propagation using non-rigid registration in the context of prostate cancer radiotherapy has been investigated. It has been shown that the non-rigid CT/CBCT registration procedure can be improved by adding a constraint term. More particularly, a rigid

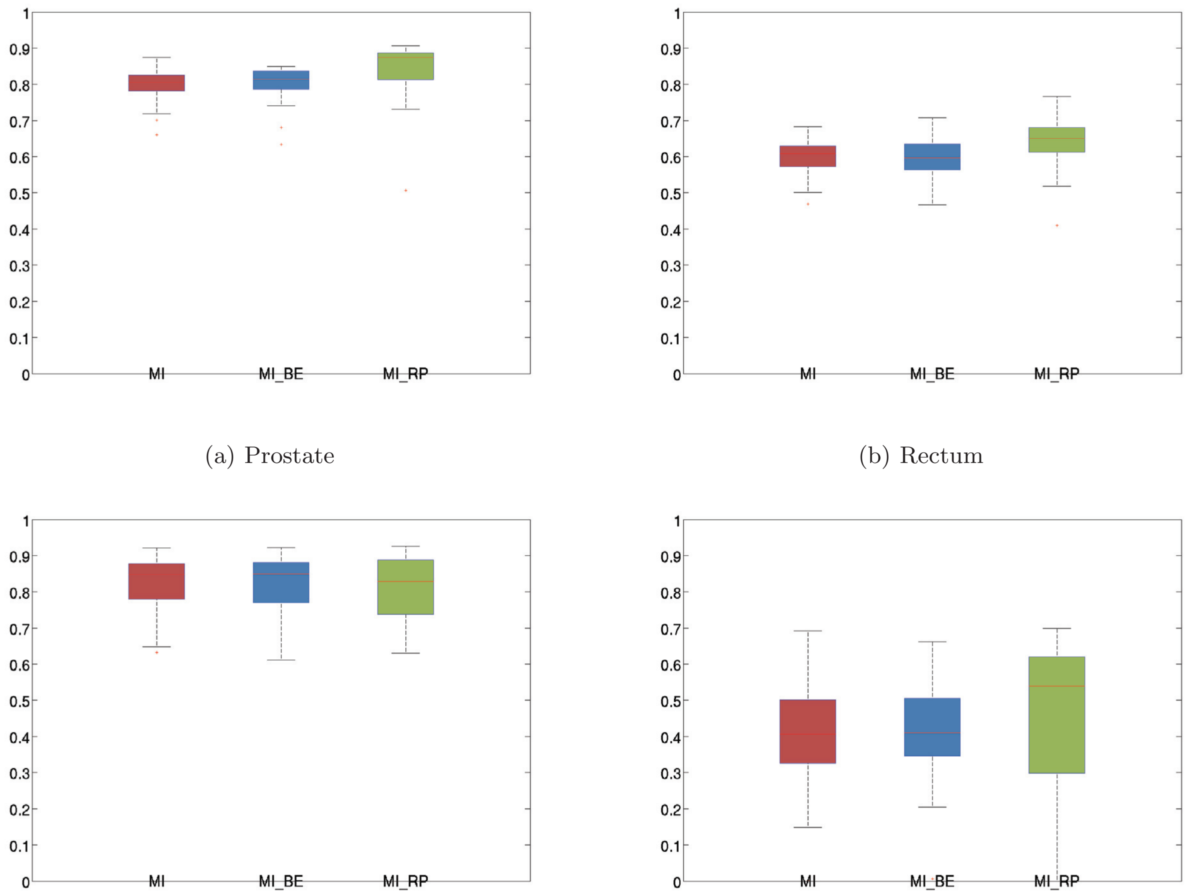

(a) Prostate (b) Rectum

(c) Bladder (d) Seminal Vesicles

Figure 2. Box plots representing the DSC obtained for the different organs under study, and for the different registration procedures used. These DSC were obtained using the original expert delineations and the ones that are propagated using the registration results. Except for the bladder (c), the procedure using a rigid penalty term on the bones always performs better on average.

penalty term placed on the bones, which are very informative structures in the considered images, can slightly improves the results by preventing undesirable foldings forcing the registration procedure to focus on the prostate and OARs. This has to be confirmed using a larger dataset and especially using other criteria to evaluate the registration procedure. This will allow to validate a registration scheme for automatic delineation propagation in prostate IGRT.

REFERENCES

[1] Greene, W., Chelikani, S., Purushothaman, K., Knisely, J., Chen, Z., Papademetris, X., Staib, L., and Duncan, J., "Constrained non-rigid registration for use in image-guided adaptive radiotherapy," *Medical image analysis* **13**(5), 809–817 (2009).

[2] Lu, C., Chelikani, S., Papademetris, X., Knisely, J. P., Milosevic, M. F., Chen, Z., Jaffray, D. A., Staib, L. H., and Duncan, J. S., "An integrated approach to segmentation and nonrigid registration for application in image-guided pelvic radiotherapy," *Medical Image Analysis* **15**(5), 772–785 (2011).

[3] Klein, S., Staring, M., Murphy, K., Viergever, M., and Pluim, J., "elastix: a toolbox for intensity-based medical image registration," *IEEE Transactions on Medical Imaging* **29**(1), 196 – 205 (2010).

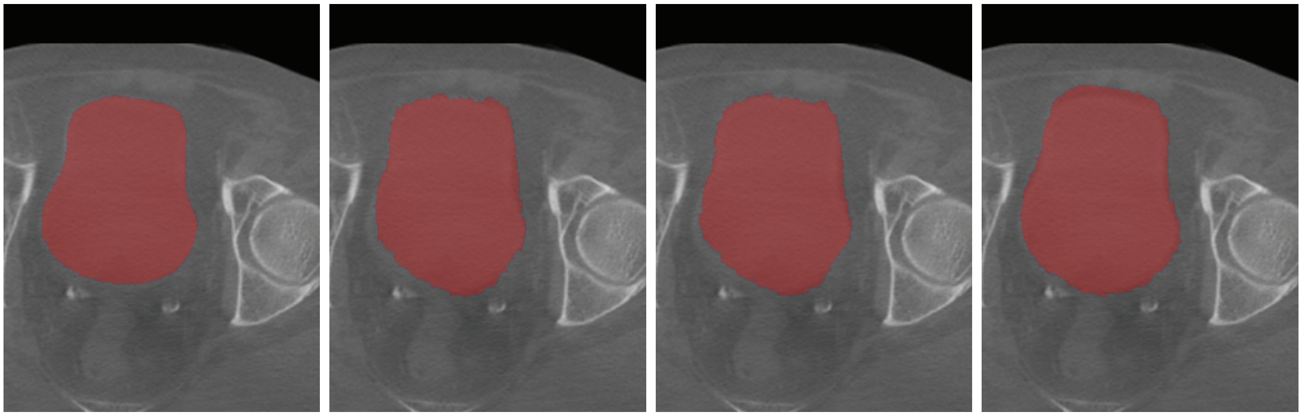

(a) Expert delineation (b) MI propagated delineation (c) MI_{BE} propagated delineation (d) MI_{RP} propagated delineation

Figure 3. Comparison between the reference expert delineation of the bladder (a) and the propagated delineation after registration with MI (b), MI_{BE} (c) and MI_{RP} (d).

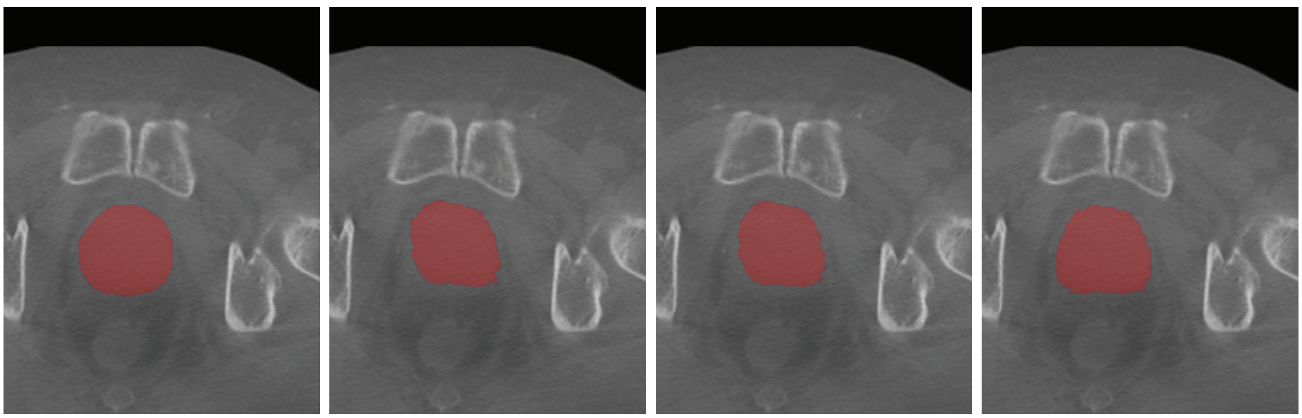

(a) Expert delineation (b) MI propagated delineation (c) MI_{BE} propagated delineation (d) MI_{RP} propagated delineation

Figure 4. Comparison between the reference expert delineation of the prostate (a) and the propagated delineation after registration with MI (b), MI_{BE} (c) and MI_{RP} (d).

[4] Thévenaz, P. and Unser, M., "Spline pyramids for inter-modal image registration using mutual information," in [*Proceedings of the SPIE Conference on Mathematical Imaging: Wavelet Applications in Signal and Image Processing V*], **3169**, 236–247 (July 30-August 1, 1997).

[5] Mattes, D., Haynor, D. R., Vesselle, H., Lewellen, T. K., and Eubank, W., "PET-CT image registration in the chest using free-form deformations.," *IEEE Transactions on Medical Imaging* **22**(1), 120–128 (2003).

[6] Rueckert, D., Sonoda, L., Hayes, C., Hill, D., Leach, M., and Hawkes, D., "Nonrigid, registration using Free-Form Deformations: Application to breast MR images," *IEEE Transactions on Medical Imaging* **18**, 712–721 (Aug. 1999).

[7] Staring, M., Klein, S., and Pluim, J., "A Rigidity Penalty Term for Nonrigid Registration," *Medical Physics* **34**, 4098 – 4108 (November 2007).

[8] Klein, S., Pluim, J., Staring, M., and Viergever, M., "Adaptive stochastic gradient descent optimisation for image registration," *International Journal of Computer Vision* **81**(3), 227–239 (2009).